# Limiter for the early operation phase of W7-X

S.A. Bozhenkov[1], F. Effenberg[2], Y. Feng[1], J. Geiger[1],
D.A. Hartmann[1], H. Hölbe[1], T.S. Pederson[1], R.C. Wolf[1]
[1] *Max Planck Institute for Plasma Physics, Wendelsteinstr. 1, 17491 Greifswald, Germany*
[2] *Institute of Energy and Climate Research, Forschungszentrum Jülich, 52425 Jülich, Germany*

## Introduction

Wendelstein 7-X [1] is an optimized modular stellarator to come into operation in 2015. In the first operational phase [2] discharges of up to 1 s with ECRH heating of at least 2 MW, possibly up to 4 MW, will be targeted. The machine will be equipped with a limited set of in-vessel components and will use a dedicated limiter configuration. In this paper the magnetic configuration is presented and the limiter design is explained. Tolerances are also discussed.

## Magnetic configuration

According to the design the W7-X stellarator has an island divertor consisting of 10 units in five modules [3]. In the standard configuration a 5/5 island chain is in contact with graphite targets, figure 1.1. Other plasma facing components are graphite baffles, inboard graphite shield, and outboard steel panels. In the first operational phase the graphite components will not be installed, figure 1.2. Consequently, metallic parts can be potentially exposed to plasma. The most critical ones are steel target support frames and CuCrZr shield cooling. To guaranty the machine safety and a reasonable performance a limiter configuration is proposed for this campaign. Because of an easy access and mounting 5 limiters are decided to be installed in symmetry planes $\varphi = 0$ onto the CuCrZr structure. To meet the requirements a magnetic configuration without big islands in the scrape-off layer (SOL) is desirable. In addition, $\iota = 1$ flux surface should be avoided to escape resonance effects of 1/1 and 2/2 field errors. A suitable configuration can be created by using W7-X planar coils to lower the angle of rotational transform $\iota$. In the standard configuration, figure 1.1, the planar coils A and B are not used: $I_{A,B} = 0$. As current $I_{A,B}$ is raised, $\iota$ is reduced and the main resonance is shifted outwards. For example, for $I_{A,B}$ equal to 0.07 relative to non-planar coils the main islands are shifted deep into the SOL: gray flux surfaces beyond the last closed flux surface (LCFS) in figure 1.2. For the early operation phase the coil current of 0.13 will be used, which results in $\iota = 1$ surface and the 5/5 islands being not in the space between the LCFS and the first wall, figure 1.3. The LCFS is determined by the limiter position described here as distance between the limiter front and the CuCrZr. From field line diffusion simulations, see the next section, the power fraction reaching the first wall, mainly the divertor frames, decreases exponentially with the limiter depth, figure 1.4. At the same time plasma radius decrease by about 2 cm per every 1 cm shift. As a compromise the limiter position of 9 cm is fixed, for which the wall fraction is below 1% and the effective radius $a$ is about

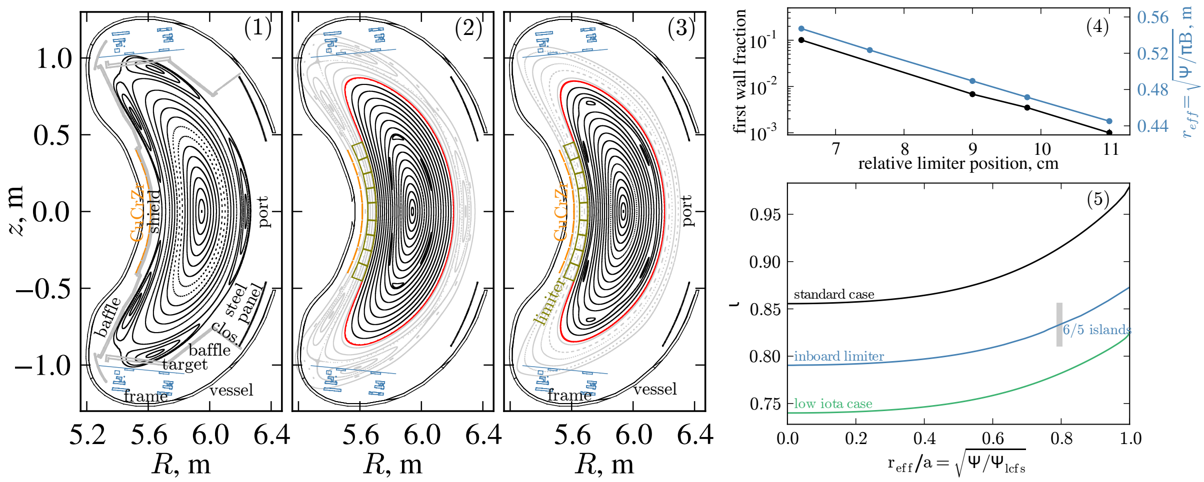


Figure 1: Magnetic configuration. **1–3** - Poincaré plots in $\varphi = 0$ plane, plasma facing components are labeled. **1** - standard 5/5 configuration. **2** - planar coils current $I_{A,B} = 0.07$. **3** - limiter configuration, $I_{A,B} = 0.13$. **4** - first wall power fraction and plasma radius vs. the limiter position. **5** - iota-profiles.

0.49 m. $\iota$-profile for the chosen configuration is presented in figure 1.5 in comparison to that for two W7-X reference cases. The limiter profile lies between the standard and the low-$\iota$ cases. For the limiter configuration a 6/5 island chain is present in the plasma at normalized radius $r_{eff}/a$ of about 0.8. These islands do not compromise the safety or the limiter performance, since they have a sufficient clearance to the LCFS and are not resonant to the main field errors.

**Limiter shape**

Limiter design is based on the assumption that the transport is convective parallel to the field and is diffusive perpendicular to that. Perpendicular diffusion coefficient $D_\perp$ is assumed to be 1 m$^2$/s. Furthermore, the ion temperature at the edge is taken to be 100 eV, which for He results in velocity $v_{||}$ of about $5 \cdot 10^4$ m/s. Helium plasmas will be used in the first part of the campaign. To simulate heat fluxes Monte-Carlo field line diffusion is applied [4]: field lines from inside the LCFS are traced with an additional artificial perpendicular diffusion.

First consider the limiter shape in a plane parallel to the field. Assuming an exponential radial power decay, the shape can be chosen is such a way as to keep the heat flux constant:

$$F_0 \cdot e^{y/\lambda} \cdot \sin\alpha = \Phi \tag{1}$$

$F_0$ is a parallel flux at LCFS, which depends on the heating power. $\Phi$ is the desired heat flux, assumed 10 MW/m$^2$. $\alpha(y)$ - angle between field lines and the limiter surface, $y$ - distance from the LCFS (negative). Decay length $\lambda$ is determined with field line diffusion for an arbitrary limiter shape. From the statics of the hit events versus the distance to the LCFS, figure 2.1, a value of about 1.5 cm is found. $F_0$ is taken for 5 MW heating power, i.e. the maximal possible installed heating of 4 MW with a safety margin. The corresponding ideal shape is presented in figure 2.2 in gray. This shape provides a limiter operation with the heat flux not exceeding

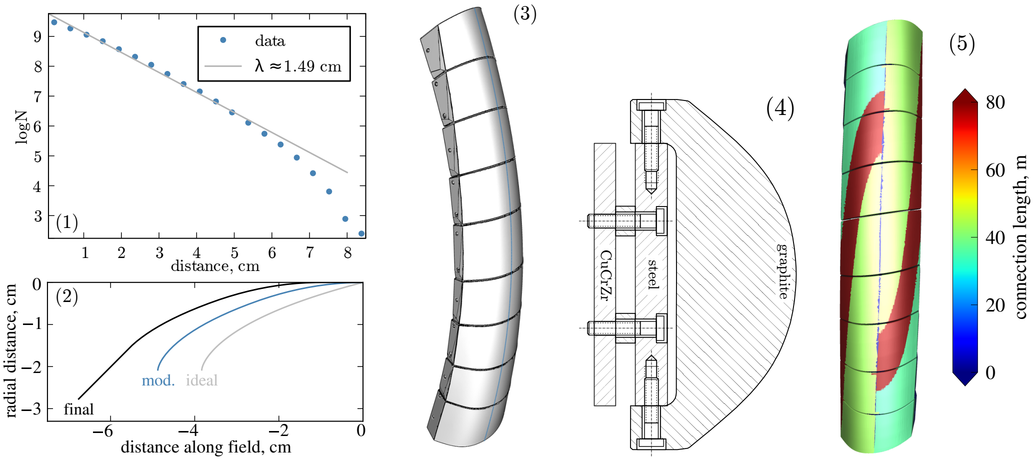


Figure 2: Limiter shape. **1** - power decay length from field line diffusion. **2** - limiter shape (half) in a plane parallel to field. **3** - 3d limiter shape. **4** - limiter side mounting. **5** - connection length on the limiter.

10 MW/m$^2$ for $D_\perp = 2$ m$^2$/s with heating of about 4 MW. To achieve the same for $D_\perp = 0.5$ m$^2$/s the central part of the limiter has to be modified, e.g. by inserting a parabolic part from the point where $\Phi$ is not exceeded, blue curve in 2.2. For technical reasons to simplify mounting, it is necessary to extend the limiter further, black curve in figure 2.2. This is implemented by adding a 2 cm plateau in the center and by applying a linear extrapolation from $\alpha = 45^\circ$ at the edge. The limiter shape in 3d is generated in the following way. The LCFS is described in magnetic coordinates [4]. Radial shifts are applied along local surface normals according to the distance from the $\varphi = 0$ plane along field lines. The resulting limiter surface is cut into 9 tiles, figure 2.3. To avoid plasma interaction with metallic screws the limiter tiles are side mounted to an adapter steel plate, the latter being fixed to the CuCrZr structure, figure 2.4. The limiter exhibits zones of different connection lengths, figure 2.5. Field lines initiating from one of them meet the next limiter after a single toroidal turn, whereas those from the other complete about 2 toroidal turns. Therefore, in reality the heat flux to the limiter is expected to be non-uniform. This is indeed found with field line diffusion, figure 3.2. The artificially introduced extensions in the center and at the edge are not loaded. In the loaded stripes one observes a poloidal asymmetry. In the regions with long connection length the heat flux is higher than otherwise by up to 20%.

**Tolerances**

Relative positioning of the limiters can be performed with an error of about 2 mm. In the worst case a single limiter is shifted by this value. Field line diffusion predicts for such a situation that the change of the heat flux is moderate: an increase of the total power and of the peak flux by about 12%. This result is consistent with the fact that the shift is much smaller than the decay length $\lambda$. Similarly, in the case of one limiter rotated by 1° along a vertical axis at the mounting plane the heat flux increase is even smaller than 10%. In the case of statistically distributed

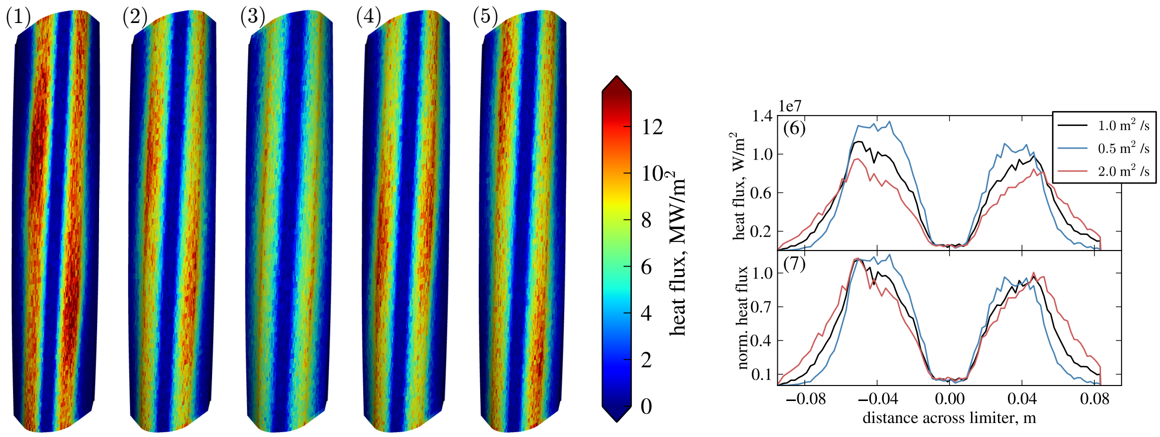


Figure 3: Heat flux simulation. **1** - $I_{A,B} = 0.13$, $D_\perp = 0.5$ m$^2$/s. **2** - $I_{A,B} = 0.13$, $D_\perp = 1.0$ m$^2$/s. **3** - $I_{A,B} = 0.13$, $D_\perp = 2.0$ m$^2$/s. **4** - $I_{A,B} = 0.10$, $D_\perp = 1.0$ m$^2$/s. **5** - $I_{A,B} = 0.16$, $D_\perp = 1.0$ m$^2$/s. **6** - horizontal slices for cases **1–3**, $0.16 < z < 0.21$ m. **7** - the same as **6**, but normalized.

errors the effect is even more benign. If the diffusion coefficient differs form the design one, the heat flux distribution changes. If the coefficient is smaller than the design one, the heat flux increases, figure 3.1, and vice versa figure 3.3. This is summarized in figures 3.6 and 3.7, where the heat flux and the normalized flux are shown across the limiter for three diffusion coefficients. From figure 3.7, from the heat flux pattern one can determine the diffusion coefficient. Such measurements will be performed with the aid of IR cameras and Langmuir probes. In the case the current in the planar coils is changed, the heat flux pattern is shifted poloidally, figures 3.4 and 3.5, due to a change in connection lengths. The peak flux remains approximately constant. An 1/1 error field changes the heat flux distribution even without a resonance. For a normalized error field of $10^{-4}$ a change of about 30% is expected. Details will be reported elsewhere.

**Summary**

In the first experimental campaign the W7-X stellarator will be a limiter machine. A dedicated magnetic configuration is created by decreasing the angle of rotational transform $\iota$ with planar coils. In this configuration the $\iota = 1$ flux surface is not present in the plasma. 5 inboard limiters will be installed in the symmetry planes $\varphi = 0$. The shape of the limiters is designed to have a heat flux of 10 MW/m$^2$ for 5 MW heating. Limiter performance is verified with field line diffusion. Installation tolerances are predicted to have a negligible effect. Thermal analysis of the assembly shows that 1 s pulses of 2 MW are allowed every 7 min and for 5 MW every 14 min. The inboard limiter provides a good opportunity to study the edge physics: measurements of the power decay length, study of effects of error fields. Limiters will be observed with IR cameras and will be equipped with Langmuir probes. Further studies of the inboard limiter are given in [5, 6].

[1] J. Geiger et al., this conference
[2] T.S. Pedersen et al., this conference
[3] J. Kißlinger et al. EPS 1994
[4] S.A. Bozhenkov et al. Fus. Eng. Design **88**, 2997
[5] Y. Feng et al., this conference
[6] F. Effenberg et al., this conference